Electronic Supplementary Material (ESI) for Green Chemistry.

Supporting Information

CoO_xH_y/β-NiOOH Electrocatalyst for Robust Ammonia Oxidation to Nitrite and Nitrate

Sam Cohen[a,b], Sam Johnston[a], Cuong Nguyen[a], Tam D. Nguyen[a], Dijon A. Hoogeveen[a], Daniel Van Zeil[a], Sarbjit Giddey[b], Alexandr N. Simonov[a], Douglas R. MacFarlane[a]

[a.] *School of Chemistry, Monash University, Clayton, VIC 3800, Australia*
[b.] *CSIRO Energy, Private Bag 10, Clayton South, Victoria 3169, Australia*

Index

Supporting Information

Figure S1. Voltammetric formation of β-NiOOH/Ni

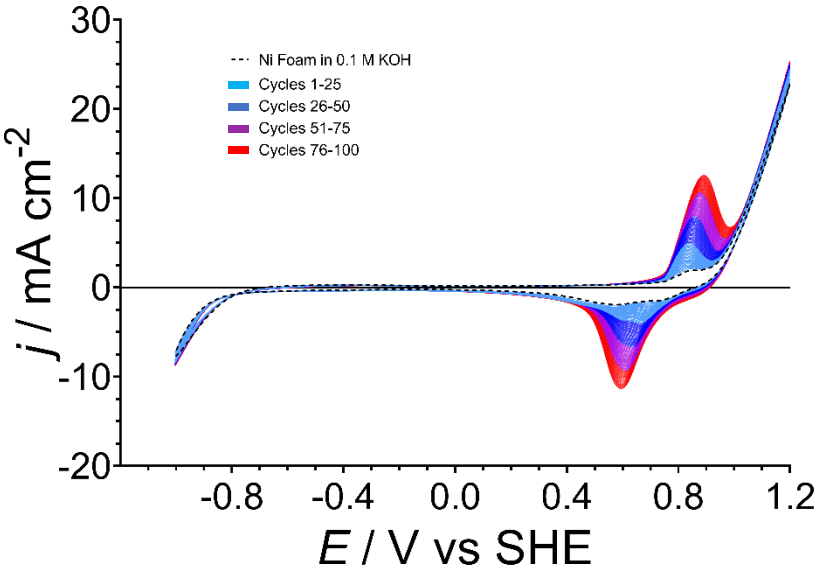

Figure S1. Averaged cyclic voltammograms (v = 0.050 V s^{-1}) for n = 3 independent nickel foam electrodes recorded in air-saturated 0.1 M KOH showing the irreversible growth of β-NiOOH over 100 cycles between -1 to 1.2 V *vs*. SHE. Growth of the β-phase of NiOOH can be observed progressing from the dotted black line (first cycle) to light blue (cycles 1-25) to dark blue (cycles 26-50), to purple (cycles 51-75). In the final stages (red, cycles 76-100), the rate of growth slows as it reaches a stable final state. Currents are normalised to the geometric surface area of the electrodes (1 cm^2).

Figure S2. Electrodeposition of CoO_xH_y onto β-NiOOH/Ni

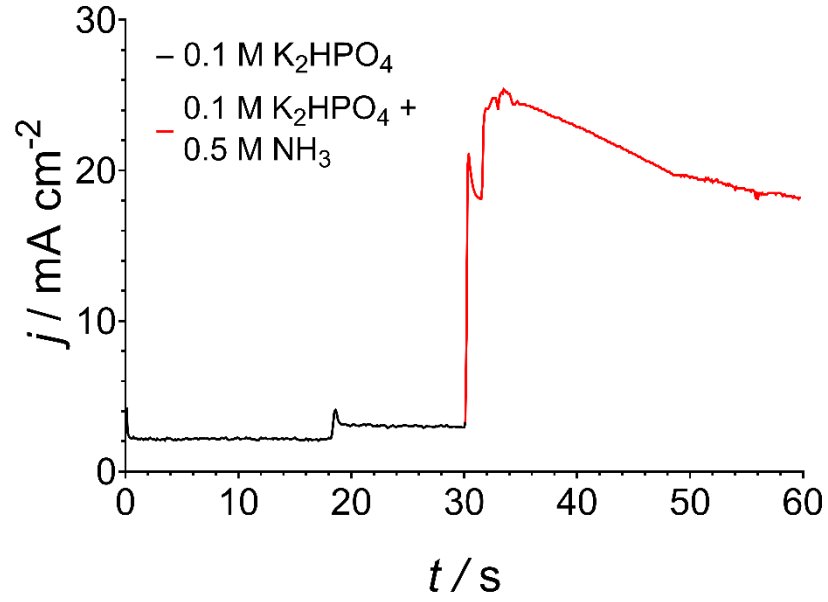

Figure S2. Chronoamperogram for the electrodeposition of cobalt (hydr)oxides/oxyhydroxides onto a β-NiOOH/Ni foam electrode recorded in 0.1 M Na_2SO_4 at 1 V *vs*. SHE. The black line shows the first stage of deposition with no ammonia present, and the red line represents the response after injecting 0.5 M NH_4OH at 30 s. Currents are normalised to the geometric surface area of the electrode (1 cm^2).

Supporting Information

Figure S3. Comparisons of the electrochemical data for Ni foam, β-NiOOH/Ni, and CoO_xH_y/β-NiOOH/Ni electrodes

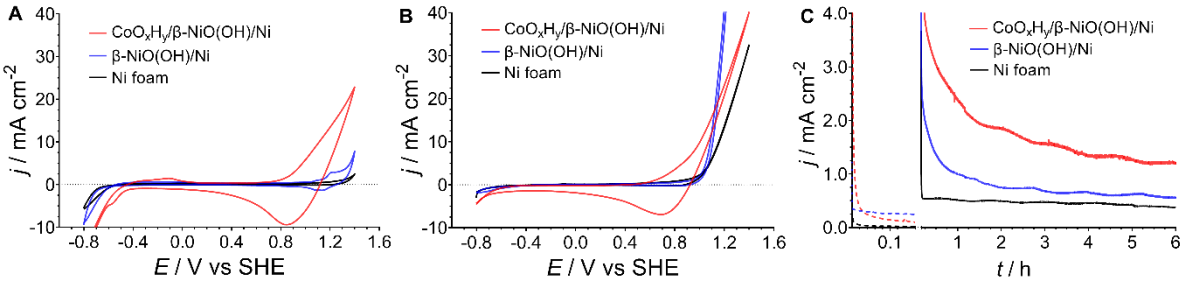

Figure S3. (A-B) Cyclic voltammograms (v = 0.050 V s^{-1}; 3rd cycles), and (C) chronoamperograms (E = 1.000 ± 0.003 V *vs*. SHE) recorded for the nickel foam, β-NiOOH/Ni and CoO_xH_y/β-NiOOH/Ni electrodes in 0.1 M K_2HPO_4 (A, C) without and (B, C) with 0.5 M NH_3 present. In panel (C), 0.5 M NH_3 was introduced after 10 min. The dotted lines represent the chronoamperograms without 0.5 M NH_3 present in this first 10 min. Currents are normalised to the geometric surface area of the electrodes (1 cm^2); data are presented as average derived from tests of n = 3 independent electrodes of each type. The same data, but in a different layout, are presented in the main text Figure 2.

Figure S4. Delamination of electrodeposit from CoO_xH_y/Ni

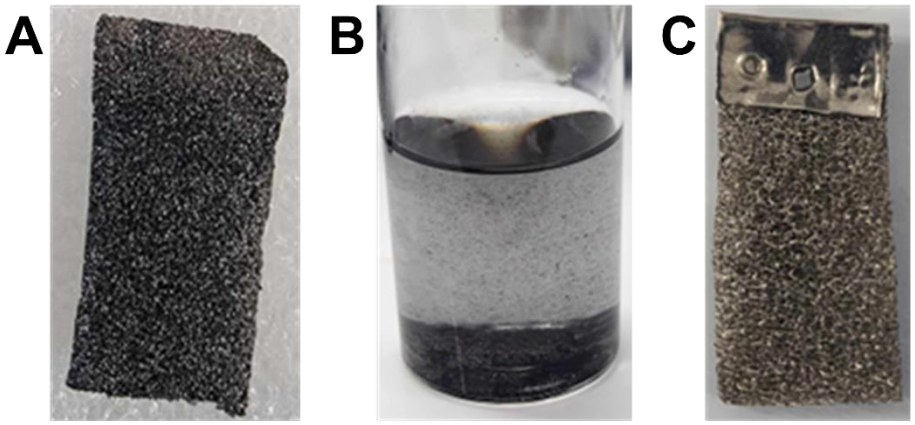

Figure S4. Photographs showing delamination of the electrodeposit from CoO_xH_y/Ni upon immersion into aqueous 0.5 M NH_3 + 0.1 M KOH for 5 min: (A) as-prepared electrode, (B) exfoliated electrodeposit particles suspended in the solution, (C) electrode after contact with the solution.

Supporting Information

Figure S5. EDS of CoO_xH_y on untreated Ni foam

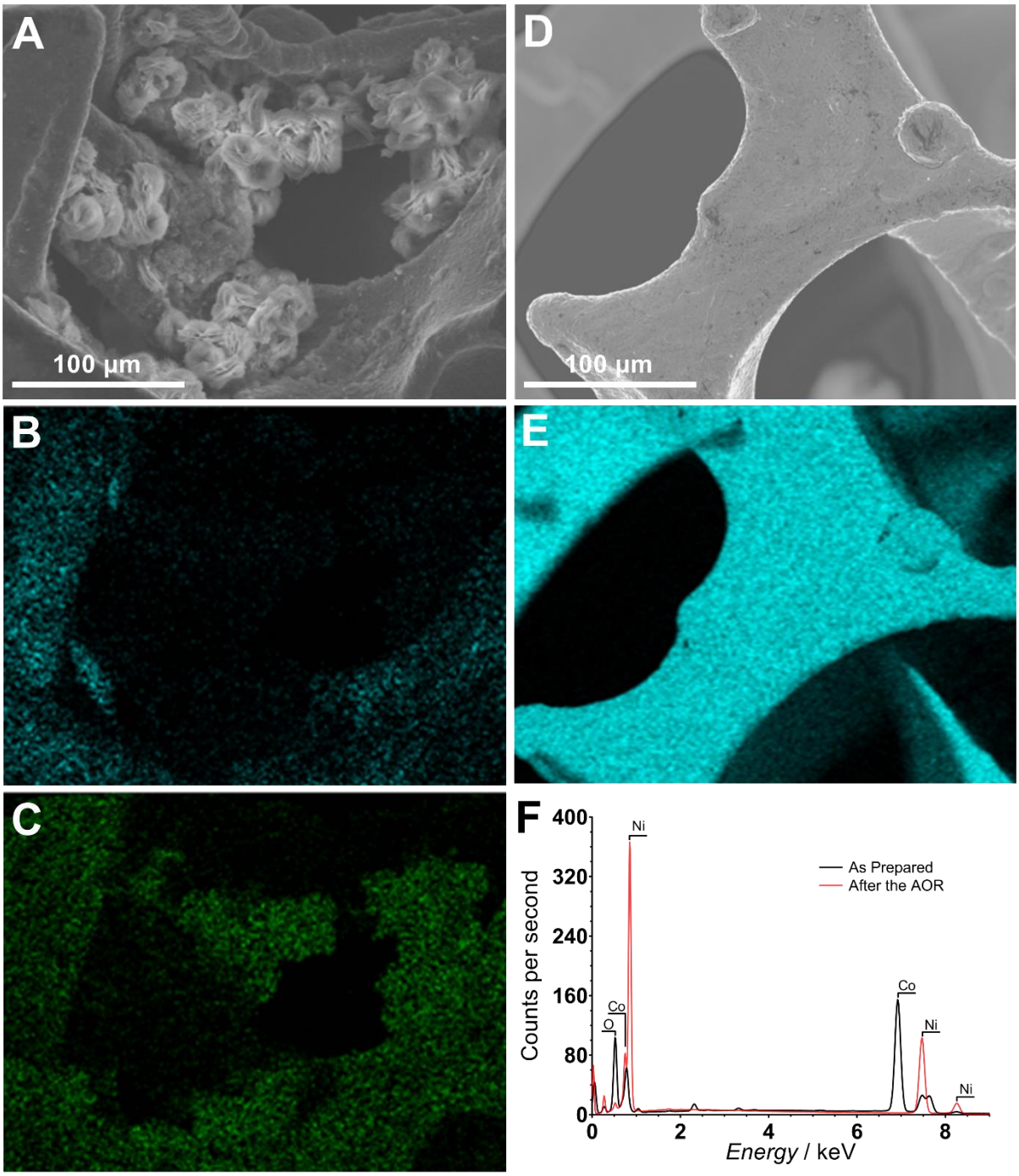

Figure S5. EDS/SEM mapping of a CoO_xH_y/Ni electrode (A-C) before and (D-E) after 6 hours of a chronoamperometric test at 1.000 ± 0.003 V *vs*. SHE in 0.1 M K_2HPO_4 + 0.5 M NH_3: (A, D) SEM micrographs, (B, E) Ni distribution, (C) Co distribution, (F) EDS map sum spectra as prepared (black) and after (red) the AOR through chronoamperometric tests. No Co EDS mapping was undertaken for the sample after test as no Co was detected (see panel F).

Supporting Information

Figure S6. Custom reference electrode

As explained in the experimental section, a custom reference electrode was required for this study. Under alkaline conditions and in the presence of ammonia, particularly with long-term experimental exposure, standard Ag|AgCl-based electrodes were expectedly damaged and unstable. These issues were circumvented by introducing a short, solid-state agarose gel salt bridge featuring a junction point between the fritted end of a standard Ag|AgCl/$KCl_{(sat.)}$ electrode and the salt bridge (Figure S6). The 'sensing end' of the salt bridge was then conditioned in 0.1 M K_2HPO_4 in order to minimise any junction potentials that may be present during operation, as well as negate any concerns surrounding silver ion or chloride leakage into the working electrolyte solution. The potential of this reference system was recorded against that of the saturated calomel electrode (SCE; E = 0.248 V *vs.* SHE) prior to and after completion of electrochemical experiments. Over more than 6 months of regular use, the potential remained highly stable at an average value of 0.191 ± 0.003 V *vs*. standard hydrogen electrode (SHE) at an average temperature 21 ± 2 °C.

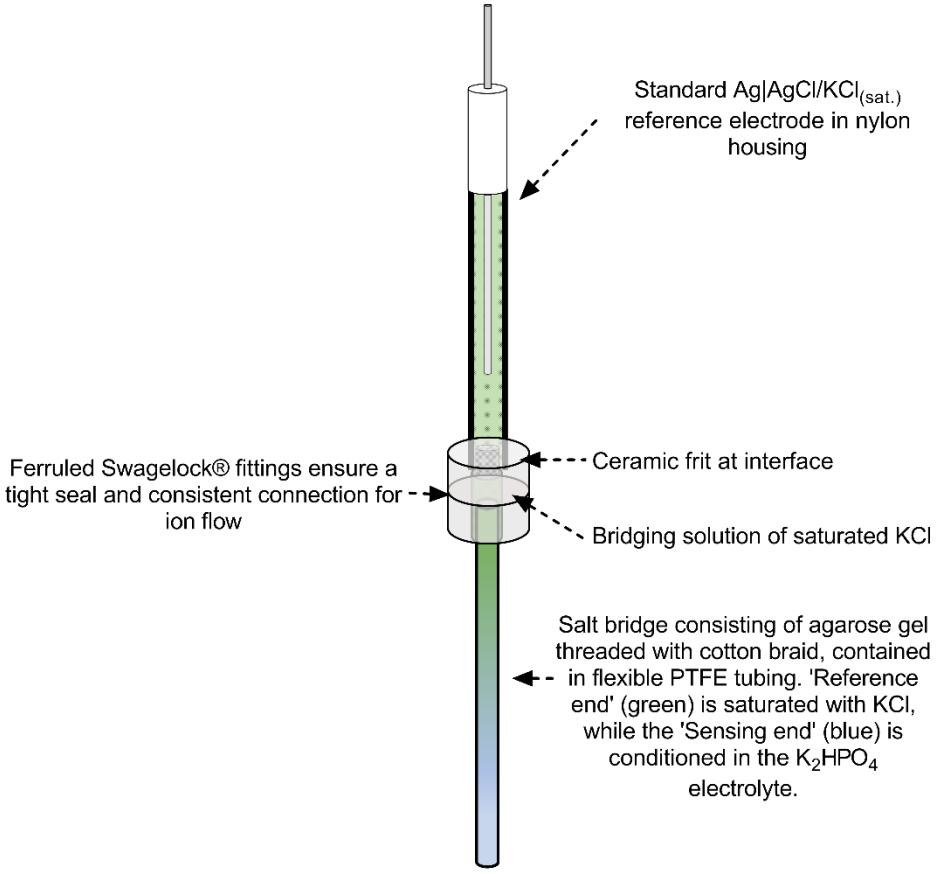

Figure S6. Schematic diagram of the reference electrode design used throughout this study.

Supporting Information

Table S1. Short-term AOR to $[NO_{2/3}]^-$ metrics at different potentials

Table S1. Faradaic efficiency and $[NO_{2/3}]^-$ yield rates during the AOR catalysed by CoO_xH_y/β-NiOOH/Ni at different potentials.[a]

E / V *vs.* SHE	$[NO_{2/3}]^-$ faradaic efficiency / %	Yield rate / nmol s^{-1} cm^{-2}	
		NO_2^-	NO_3^-
0.8	0	0	0
0.9	19	0.2	0
1.0	28	4.5	1.5
1.1	26	3.2	2.4
1.2	26	5	2.7
1.3	22	5.3	2.6

[a] Data were derived from 10 min chronoamperometric tests in 0.1 M K_2HPO_4 + 0.5 M NH_3 of 1 cm^2 electrodes.

Table S2. Greenhouse gas analysis

Table S2. Concentration of N_2O, CO_2 and CH_4 in the gas headspace before and after ammonia electrooxidation.[a]

Gas	Concentration / ppm	
	t = 0	*t* = 24 h
N_2O	0.49	0.50
CO_2	590	600
CH_4	3.3	3.1

[a] Tests were undertaken at a constant potential of 1.0 V *vs.* SHE using continuously stirred 0.1 M K_2HPO_4 + 0.5M NH_3 using 1 cm^2 CoO_xH_y/β-NiOOH/Ni electrodes inside a gas-proof cell. Aliquots of the headspace (2.5 mL) were analysed by gas chromatography using thermal conductivity (CO_2), flame ionisation (CH_4) and electron capture (N_2O) detectors.

Table S3. NH_3 oxidation by dissolved O_2

Table S3. Catalytic activity of CoO_xH_y for the NH_3 oxidation by dissolved O_2.[a]

Product	Yield / µmol	Yield Rate / nmol s^{-1} mg^{-1}
NO_2^-	5 ± 2	0.02 ± 0.01
NO_3^-	52 ± 5	0.24 ± 0.10

[a] Experiments were undertaken over 6 hours of continuous stirring of dispersions of CoO_xH_y powder (1 mg mL^{-1}) detached from the CoO_xH_y/β-NiOOH/Ni electrodes in air-saturated 0.1 M K_2HPO_4 + 0.5 M NH_3. Data are shown as mean ± standard deviation for tests of *n* = 3 independent samples.

Supporting Information

Table S4. Summary of the key AOR performance metrics in 6 hour tests

Table S4. Performance of Ni, β-NiOOH/Ni and CoO_xH_y/β-NiOOH/Ni electrodes for the AOR.[a]

Electrode	Yield / μmol		Charge / C	Faradaic efficiency / %		Yield Rate / nmol s^{-1} cm^{-2}		Dissolution Rate / nmol s^{-1}	
	NO_2^-	NO_3^-		NO_2^-	NO_3^-	NO_2^-	NO_3^-	Ni	Co
Ni	2.7 ± 0.2	0.7 ± 0.5	11.4 ± 1.2	13.7 ± 1.3	5 ± 3	0.10 ± 0.01	0.04 ± 0.02	4.4 ± 0.5	n.a.[b]
β-NiOOH/Ni	4.1 ± 1.3	3.6 ± 0.6	18.2 ± 1.2	13 ± 5	16 ± 4	0.2 ± 0.1	0.20 ± 0.03	545 ± 1	n.a.
CoO_xH_y/β-NiOOH/Ni	17 ± 5	15 ± 7	30 ± 8	38 ± 5	41 ± 10	0.8 ± 0.2	0.7 ± 0.3	0.3 ± 0.2	0.4 ± 0.2

[a] Data were derived from 6 hour chronoamperometric tests at 1.000 ± 0.003 V *vs.* SHE in 0.1 M K_2HPO_4 + 0.5 M NH_3 for n = 3 independent samples of each type and are presented as mean ± standard deviation; geometric electrode surface area was 1 cm^2 in all cases. [b] Not applicable.

Supporting Information

Table S5. Corrosion of CoO_xH_y/β-NiOOH/Ni during the AOR

Table S5. Amount of Co and Ni dissolved from CoO_xH_y/β-NiOOH/Ni during the AOR tests.[a]

Time / h	Dissolved metal / μmol cm^{-2}	
	Ni	Co
6	6.8 ± 0.3	7.5 ± 0.2
96	8.3 ± 0.7	28.5 ± 1.2

[a] Data were derived from the ICP-MS analysis of the electrolyte solutions after chronoamperometric tests of 1 cm^2 CoO_xH_y/β-NiOOH/Ni electrodes at 1.000 ± 0.003 V *vs.* SHE in 0.1 M K_2HPO_4 + 0.5 M NH_3. Three independent samples were used for 6 hour tests, and the data are presented as mean ± standard deviation. One 96 h experiment was undertaken; error in this case represents average of *n* = 3 ICP-MS measurements.